Environmental Microbiology (2018) **00**(00), 00–00 doi:10.1111/1462-2920.14345

Increases in temperature and nutrient availability positively affect methane-cycling microorganisms in Arctic thermokarst lake sediments

Anniek E. E. de Jong,[1,2†] **Michiel H. in 't Zandt**,[1,2†] **Ove H. Meisel**,[2,3] **Mike S. M. Jetten**,[1,2,4] **Joshua F. Dean**,[2,3] **Olivia Rasigraf**[1,2] **and Cornelia U. Welte**[1,4*]

[1]*Department of Microbiology, Institute for Water and Wetland Research, Radboud University, Heyendaalseweg 135, 6525 AJ Nijmegen, The Netherlands.*

[2]*Netherlands Earth System Science Center, Utrecht University, Heidelberglaan 2, 3584 CS Utrecht, The Netherlands.*

[3]*Department of Earth Sciences, Vrije Universiteit Amsterdam, De Boelelaan 1085, 1081 HV Amsterdam, The Netherlands.*

[4]*Soehngen Institute of Anaerobic Microbiology, Radboud University, Heyendaalseweg 135, 6525 AJ Nijmegen, The Netherlands.*

Summary

Arctic permafrost soils store large amounts of organic matter that is sensitive to temperature increases and subsequent microbial degradation to methane (CH_4) and carbon dioxide (CO_2). Here, we studied methanogenic and methanotrophic activity and community composition in thermokarst lake sediments from Utqiaġvik (formerly Barrow), Alaska. This experiment was carried out under *in situ* temperature conditions (4°C) and the IPCC 2013 Arctic climate change scenario (10°C) after addition of methanogenic and methanotrophic substrates for nearly a year. Trimethylamine (TMA) amendment with warming showed highest maximum CH_4 production rates, being 30% higher at 10°C than at 4°C. Maximum methanotrophic rates increased by up to 57% at 10°C compared to 4°C. 16S rRNA gene sequencing indicated high relative abundance of *Methanosarcinaceae* in TMA amended incubations, and for methanotrophic incubations *Methylococcaceae* were highly enriched. Anaerobic methanotrophic activity with nitrite or nitrate as electron acceptor was not detected. This study indicates that the methane cycling microbial community can adapt to temperature increases and that their activity is highly dependent on substrate availability.

Received 3 April, 2018; revised 27 June, 2018; accepted 27 June, 2018. *For correspondence. E-mail c.welte@science.ru.nl; Tel. +31 24 3652952. †These authors contributed equally to this work.

Introduction

In Arctic and sub-Arctic ecosystems, thermokarst lakes cover about 20%–40% of the permafrost regions (Osterkamp *et al*., 2009; Koch *et al*., 2014; Abbott *et al*., 2015; Schuur *et al*., 2015; Narancic *et al*., 2017). Thermokarst lakes evolve through horizontal and vertical permafrost degradation, which creates characteristic eroding shorelines from where sediment is slumping into the lake. These lakes are generally shallow (< 3.0 m) and range in size from a few square meters to hundreds of square kilometers (Grosse *et al*., 2013; Wik *et al*., 2016). Due to warming, there is a retreat or melting of permafrost that may result in an increase in lake numbers and expansion of their area (Karlsson *et al*., 2015). Interestingly, these thermokarst lakes contribute significantly to methane (CH_4) emissions (Walter *et al*., 2006, 2008; Olefeldt *et al*., 2016; Wik *et al*., 2016), releasing an estimated 4.1 $\pm$ 2.2 Tg CH_4 y^{-1} (Wik *et al*., 2016). With the prediction of 20 more ice-free days on Arctic water bodies before 2079 (Dibike *et al*., 2011; Prowse *et al*., 2011), CH_4 emissions from thermokarst lakes are expected to increase by 30% (Wik *et al*., 2016).

The majority of globally emitted CH_4 (60%–70%) originates from biogenic sources (Kirschke *et al*., 2013; Myhre *et al*., 2013). Methane is produced by methanogenic archaea as the terminal step of microbial decomposition of organic matter in anoxic environments. Methanogenic substrates include hydrogen/carbon dioxide (H_2/CO_2) (hydrogenotrophic methanogenesis), methylated compounds including methanol (MeOH) (methylotrophic methanogenesis), acetate (acetoclastic methanogenesis) and methoxylated aromatic compounds (methoxydotrophic methanogenesis) (Garrity *et al*., 2004; Cheng *et al*., 2007; Thauer and Shima, 2008; Dridi *et al*., 2012; Mayumi *et al*., 2016). In permafrost soils, H_2/CO_2 and

acetate are the main substrates (Kotsyurbenko *et al*., 2001; Basiliko *et al*., 2003; Nozhevnikova *et al*., 2003; Galand *et al*., 2005; Kotsyurbenko, 2005; Metje and Frenzel, 2007; McCalley *et al*., 2014; Yang *et al*., 2017), but there are contradicting reports on the respective predominant methanogenesis pathway in thawing permafrost. Several studies found an association of acetoclastic methanogenesis with thawing permafrost (Høj *et al*., 2008; Barbier *et al*., 2012; McCalley *et al*., 2014; Mondav *et al*., 2014; Blake *et al*., 2015; Coolen and Orsi, 2015; Gill *et al*., 2017; Voigt *et al*., 2017), while other data suggests an increase in hydrogenotrophic methanogenesis (Kotsyurbenko, 2005; Wagner *et al*., 2005; Kotsyurbenko *et al*., 2007; Blake *et al*., 2015; Liebner *et al*., 2015).

The produced methane diffuses through the sediment column upward, where it can be (partially) oxidized to CO_2 by methanotrophic Archaea and Bacteria. The aerobic methanotrophs in permafrost soils are generally dominated by type I methanotrophs (Gammaproteobacteria) (Trotsenko and Khmelenina, 2005; Wagner *et al*., 2005; Liebner and Wagner, 2007; Trotsenko and Murrell, 2008; Liebner *et al*., 2009; Semrau *et al*., 2010; He *et al*., 2012; Martinez-Cruz *et al*., 2017), whilst some other studies found high relative abundance of type II methanotrophs (Alphaproteobacteria) (Knoblauch *et al*., 2008; Stackhouse *et al*., 2017). Methanotrophs affiliated with Verrucomicrobia have been detected in permafrost sediments (Hansen *et al*., 2007; Dan *et al*., 2014; Ganzert *et al*., 2014; Deng *et al*., 2015; Frey *et al*., 2016). Recently, the potential for anaerobic oxidation of methane (AOM) has been shown in (submarine) permafrost (Overduin *et al*., 2015; Winkel *et al*., 2018).

CH_4 emissions from natural environments will likely increase by 2100 and beyond (Dean *et al*., 2018). However, the relative contribution of Arctic microbial methane fluxes to global methane emission remains highly uncertain (Wagner *et al*., 2017). In order to predict the vulnerability of permafrost carbon to decomposition and the resulting methane emission, we need to better understand how Arctic microbial communities respond to realistic warming scenarios and changes in nutrient availability. Identifying the responsible microbial communities is a good starting point in unravelling the microbial diversity and activity, and in quantifying the contribution of thermokarst lakes to the global methane budget in a warming world. Here, we investigate the effect of the projected temperature increase (+6°C by 2100; Myhre *et al*., 2013) on the activity and community composition of both methane-producing and -oxidizing microorganisms in the sediment of two thermokarst lakes in Utqiaġvik, Alaska. The influence of temperature on Arctic microbial communities was assessed by a complementary array of techniques including 16S rRNA gene amplicon sequencing and CH_4 flux measurements in batch incubations. We found that both methanogenic and aerobic methanotrophic rates increased with warming. The microbial community composition changed in response to the addition of different substrates.

Results

Biogeochemistry of the thermokarst lake sediments

Sediment cores were taken in duplicates from four different sites of Lake Emaiksoun and three sites from Unnamed Lake in the vicinity of Utqiaġvik, Alaska, during a winter field campaign in November 2015 (Supporting Information Table S1, Supporting Information Fig. S1). The top 30–40 cm of all cores was made up by clay-dominated silty, organic-rich (30 wt% total organic carbon), brown mud that was abruptly truncated at the bottom by a sharp boundary to the underlying sediment. These lower halves of the cores consisted of old coastal sand, pebble and silt deposits, which gradually turned into clayey marine mud toward the bottom. This sequence of marine layers documents the regression of the paleo shoreline. The associated marine and coastal deposits can be attributed to the Barrow Unit of the Gubik formation, which is a well-documented Quaternary deposit in near-coastal landscapes of northernmost Alaska (Black, 1964). Pore water sample analysis showed that total nitrogen was 8.1 mg L^{-1}, predominantly present in the form of ammonium (8 mg L^{-1}) and only trace amounts of nitrate (0.1 mg L^{-1}) (Supporting Information Tables S2 and S3). Total phosphate and sulfate were 0.8 and 1.8 mg L^{-1} respectively. The total salinity of the pore water was around 500 ppm, indicating that these thermokarst lakes are freshwater systems.

Bacterial and archaeal community composition in the lake sediments

One of the duplicate cores taken per sample site was used for further studies. For each core, the 16S rRNA genes were amplified using two distinct primer sets targeting Bacteria and Archaea and were sequenced with Illumina technology. The total abundance of Bacteria and Archaea was quantified by qPCR, and showed that Bacteria were seven times more abundant based on copy number than the Archaea in all sediment cores (Fig. 1). The bacterial community structure was similar in both lakes, which was supported by non-metric multidimensional scaling (NMDS) analysis (Supporting Information Figs. S2 and S3). Diversity analysis using the Simpson and Shannon diversity indices indicated similar diversity for the seven thermokarst lake sediment cores with higher diversity for the bacterial than the archaeal community on OTU level (Supporting Information Tables S4 and S5). This was also reflected by the Chao1 species richness

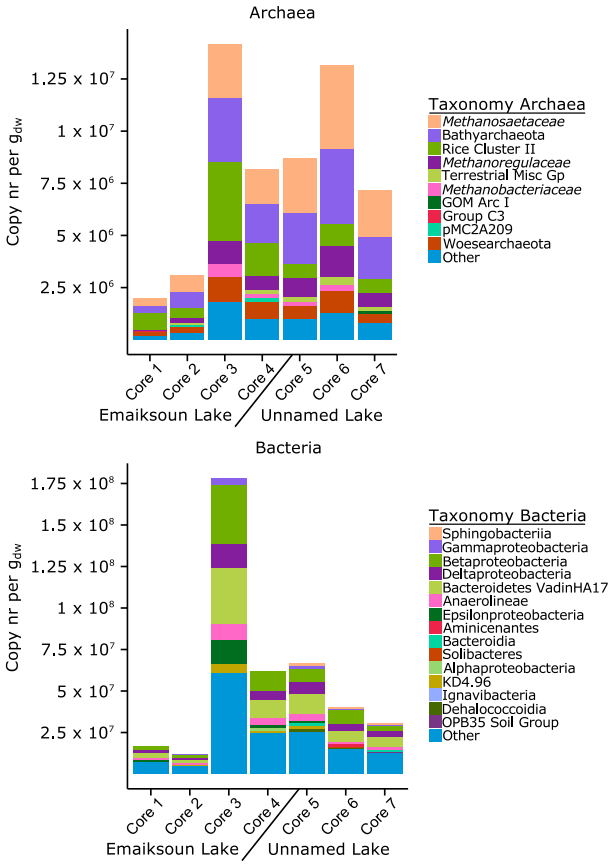

Fig. 1. Distribution of 16S rRNA gene reads of major archaeal (A) and bacterial taxonomic groups (B) in the seven thermokarst lake sediment cores. The maximum taxonomy depth is on family level for Archaea and on order level for Bacteria. Total amount of 16S rRNA gene copy number determined by qPCR amplicons per gram dry weight is depicted vertically, whereas the cores are shown horizontally. Taxonomic groups with < 2% abundance are grouped to category 'Other'.

estimation (Supporting Information Tables S4 and S5). Additionally, both Simpson- and Shannon-based evenness were similar in all cores for both the archaeal and bacterial communities (Supporting Information Tables S4 and S5). The bacterial community was very diverse (Fig. 1): a rare microbial biosphere prevailed with around 50% of the reads affiliated to groups with an individual relative abundance of less than 2%. The most abundant bacteria belonged to Bacteriodetes with 16%–19%, followed by 9%–17% assigned to Nitrosomonadales, and 4–8% of the Anaerolineales order. A difference between the lakes was observed in the relative abundance of Campylobacterales (Epsilonproteobacteria) in Lake Emaiksoun (3%–8%) compared with < 2% in Unnamed Lake. Most archaeal reads (16%–40%) in Lake Emaiksoun were affiliated to Rice Cluster II organisms, whereas *Methanosaetaceae* (30%–31%) reads showed highest relative abundance in Unnamed Lake (Fig. 1). The second most abundant phylum was Bathyarchaeota (17%–24% in Lake Emaiksoun and 27%–28% in Unnamed Lake). Woesearchaeota were present in both lakes (8%–10% in Emaiksoun Lake; 5%–8% in Unnamed Lake).

Activity and community composition of methanogens

Since bacterial and archaeal OTUs of the original sediments were similar according to diversity analyses, the thermokarst lake sediment cores (one of the duplicate sediment cores taken per sample site) were homogenized and combined prior to incubation. Methanogenic activity at 4°C and 10°C was determined for 279 days in sediment slurries amended with acetate, trimethylamine (TMA), and H_2/MeOH, and for 64 days with H_2/CO_2 (Fig. 2). In all the incubations, the CH_4 production rates were higher at 10°C than at 4°C (Table 1). At both temperatures, the substrate additions induced higher methanogenic activity over the control except for H_2/MeOH. The highest methanogenesis rates were observed with TMA as substrate with 6.6 ± 0.01 μmol CH_4 gdw^{-1} d^{-1} and 8.5 ± 0.3 μmol CH_4 gdw^{-1} d^{-1} at 4°C and 10°C respectively (Table 1). This was followed by acetate, being 3% higher at 10°C compared with 4°C. For both incubations, the total CH_4 production was not significantly different (two-sided *t*-test; $p > 0.05$). The incubation with H_2/CO_2 were active in the first 60 days but only produced substoichiometric amounts of methane. The maximum Q_{10} coefficient, which corresponds to the rate change as a result of temperature increase, for TMA, acetate and the control incubations was detected after 98 days, with values of 9.8, 4.2 and 3.3 respectively. Final Q_{10} values were 0.9, 1.1 and 1.1 for TMA, acetate and the control. For the H_2/CO_2 incubation the maximum Q_{10} coefficient of 2.0 was obtained after 52 days. Cell-specific methanogenesis rates had only minor differences between 4°C and 10°C on acetate (8.1 and 7.7 fmol $cell^{-1}$ d^{-1} for 4°C and 10°C respectively) and TMA (51 and 40 fmol $cell^{-1}$ d^{-1} for 4°C and 10°C respectively) and are all in the range of previously observed methane production rates (Supporting Information Table S6) (in 't Zandt *et al*., 2018).

The qPCR data showed that the total archaeal 16S rRNA gene copy numbers increased in all methanogenic incubations compared to the control, except for H_2/MeOH, consistent with the low methane production in this incubation (Table 2). Archaeal copy numbers in TMA amended incubations increased 19- to 28-fold compared with control incubations at 4°C and 10°C respectively, and had six-times more archaeal than bacterial copy numbers at both temperatures. In addition to the increase in archaeal copy numbers, the community composition of the archaea changed (Fig. 3). In TMA amended cultures, *Methanosarcinaceae* were the most abundant Archaea (94% of archaeal reads at 4°C, and 91% of archaeal reads at 10°C). The incubations amended with acetate contained about equal

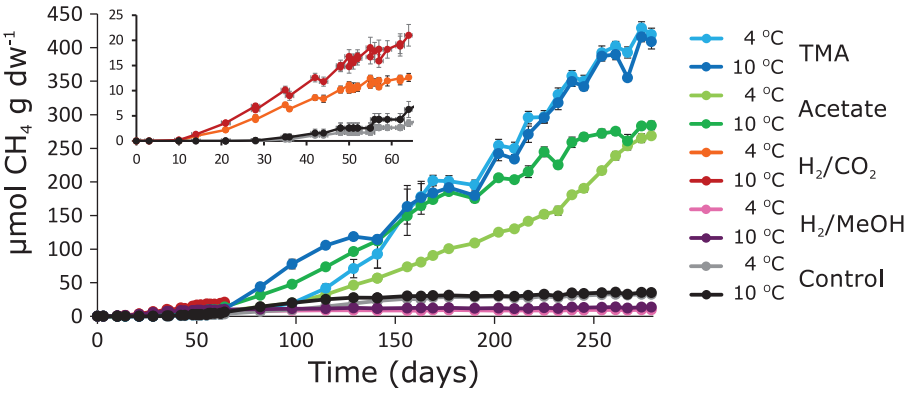

Fig. 2. CH_4 production in batch incubation assays of thermokarst lake sediment slurry at 4°C and 10°C amended with different methanogenic substrates. Each data point represents the average of three incubations. Substrates: trimethylamine (TMA), acetate, hydrogen/methanol (H_2/MeOH), H_2/CO_2, the control contained only sediment slurry. Error bars indicate standard deviation of the mean. The insert depicts the H_2/CO_2 cultures during 0–64 days.

numbers of Archaea and Bacteria at 4°C and 10°C, with *Methanosaetaceae* (51% at 4°C, and 72% at 10°C) as the most abundant archaeal group. The archaeal communities in the incubations with H_2/CO_2 and H_2/MeOH did not change much with respect to microbial community structure. In general, the bacterial community was still highly diverse in these incubations, with a similar community structure as the control (Supporting Information Fig. S4).

Activity and community composition of aerobic methanotrophs

To determine aerobic methanotrophic activity, batch incubations with original sediment were amended with CH_4 and oxygen (O_2) and CH_4 consumption was followed for 62 days (Fig. 4A). Maximum methanotrophic oxidation rates increased by up to 57% with temperature rise, from 90 ± 8 µmol CH_4 gdw^{-1} d^{-1} at 4°C to 141 ± 0.2 µmol CH_4 gdw^{-1} d^{-1} at 10°C. The Q_{10} coefficient had a maximum value of 2.6 after 46 days, indicating temperature sensitivity. The cumulative CH_4 consumption over 62 days was 2.2 ± 0.08 mmol CH_4 gdw^{-1} at 4°C and 2.5 ± 0.06 mmol CH_4 gdw^{-1} at 10°C (Fig. 4B), which indicated on average a 10% increase in CH_4 consumption rate at 10°C. Cell-specific rates were 83 and 112 fmol $cell^{-1}$ h^{-1} for 4°C and 10°C, which is within the range previously reported for aerobic methanotrophs (Supporting Information Table S6) (in 't Zandt *et al*., 2018).

Table 1. Methanogenesis rates and total methane production measured in soil slurries incubated with 2 mM trimethylamine (TMA), 2 mM Acetate, 2 mM methanol (MeOH) with 2 mM H_2 and 8 mM H_2 with 2 mM CO_2.

	Maximum methane production rate (µmol CH_4 gdw^{-1} d^{-1})		Total methane production (µmol CH_4 gdw^{-1})	
Substrate	4°C	10°C	4°C	10°C
TMA	6.6 (±0.01)	8.5 (±0.3)	420 (±9)	400 (±11)
Acetate	3.4 (±0.4)	4.7 (±0.3)	268 (±2)	278 (±6)
H_2/CO_2*	0.7 (±0.05)	1.3 (± 0.1)	13 (±1)	21 (±2)
H_2/MeOH	0.3 (±0.2)	0.7 (±0.04)	10 (±0.3)	13 (±1)
Control	1.0 (±0.07)	1.7 (±0.2)	33 (±2)	34 (±2)

As control, sediment slurries were incubated without additional substrate. Gas measurements were performed in triplicate, and rates were calculated for the linear phase. Numbers between brackets display standard deviation of the mean.
*64 days of incubation.

The 16S rRNA gene analysis (Fig. 5) showed that type I methanotrophs from the Methylococcales order dominated the enrichment cultures (20%–22% of bacterial reads). There were no reads affiliated with type II methanotrophs. The non-methanotrophic population included potentially methylotrophic Methylophilales with a relative abundance of 5%–6%. Most surprisingly, Flavobacteriales showed highest relative abundance in both methanotrophic incubations (49% at 4°C, 40% at 10°C). The community composition of the controls showed a relative dominance of the Nitrosomonadales, which are ammonia oxidizing bacteria that could grow on the ammonium (1 mM) provided as the sole nitrogen source. qPCR showed a ratio of 14:1 of bacterial to archaeal 16S rRNA gene copy number for CH_4 amended cultures (Table 3). The archaeal abundance decreased substantially, but the community composition did not change much compared to the control and the original sediments (Fig. 1; Supporting Information Fig. S5).

Anaerobic nitrite- and nitrate-dependent methane oxidation

The potential for AOM was determined by the amendment of nitrite (NO_2^-) or nitrate (NO_3^-) under anoxic conditions. Although substrates were replenished when depleted, no stimulation of anaerobic methanotrophic activity was observed, since no increase in $^{13}CO_2$ was measured in the headspace over 450 days.

Analysis of single-end reads revealed the presence of the Soil Crenarchaeotic Group

All sequencing results presented above were obtained from Illumina paired-end data. However, as 16S rRNA gene

Table 2. Quantification of archaeal and bacterial 16S rRNA gene copy number per gram dry weight in methanogenic incubations.

	Archaeal 16S rRNA gene copies per gdw		Bacterial 16S rRNA gene copies per gdw		Archaeal reads to control		Bacterial reads to control	
Substrates	4°C	10°C	4°C	10°C	4°C	10°C	4°C	10°C
TMA	8.5×10^8 ($\pm 6.7 \times 10^6$)	1.2×10^9 ($\pm 1.4 \times 10^7$)	1.5×10^8 ($\pm 3.0 \times 10^6$)	1.8×10^8 ($\pm 2.5 \times 10^6$)	19.0	28.7	0.6	1.0
Acetate	7.8×10^7 ($\pm 2.3 \times 10^6$)	1.3×10^8 ($\pm 6.6 \times 10^5$)	1.0×10^8 ($\pm 1.5 \times 10^6$)	1.4×10^8 ($\pm 3.0 \times 10^6$)	1.7	2.9	0.4	0.8
H_2/CO_2*	1.9×10^7 ($\pm 2.6 \times 10^5$)	1.6×10^7 ($\pm 9.7 \times 10^4$)	6.4×10^7 ($\pm 4.9 \times 10^6$)	7.0×10^7 ($\pm 2.4 \times 10^5$)	nd	nd	nd	nd
H_2/MeOH	1.3×10^7 ($\pm 3.7 \times 10^5$)	1.2×10^7 (± 0)	8.9×10^7 ($\pm 5.2 \times 10^5$)	6.6×10^7 ($\pm 1.3 \times 10^6$)	0.3	0.3	0.4	0.4
Control	4.5×10^7 ($\pm 4.0 \times 10^5$)	4.3×10^7 ($\pm 4.2 \times 10^5$)	2.5×10^8 ($\pm 3.3 \times 10^6$)	1.8×10^8 ($\pm 4.2 \times 10^6$)	nd	nd	nd	nd

Numbers between brackets display standard deviation of the mean. *64 days of incubation.

amplicon sequencing depends on primer-based amplification, a bias can be introduced due to primer specificity. Amplification biases may result in single-end amplification. Therefore, single-end data were analyzed separately to quantify the bias for our datasets. The single-end sequences showed the same amount of OTUs as for paired-end data, with a total input of nearly 1 million single-end reads. Single-end data indicated the presence of the Soil Crenarchaeota Group (SCG), whereas paired-end data did not. The relative abundance of SCG in the archaeal single-end reads of the original core was 22%–48%. Their relative abundance ranged between 16% and 23% for the methanogenic enrichments amended with H_2/CO_2, H_2/MeOH and the control. SCG relative abundance in acetate and TMA incubations was lower (3%–6%). For the aerobic methanotrophic cultures, between 39% and 69% of the archaeal single-end reads were affiliated to the SCG. Recently it was found that the forward primer Arc349F, mostly used for Illumina 16S rRNA gene sequencing of Archaea and also used in this study, only matches 53% of Archaea and missed almost all Crenarchaea and unclassified Archaea (Hugerth *et al*., 2014). Single-end data suggest that SCG might play an important role in this ecosystem.

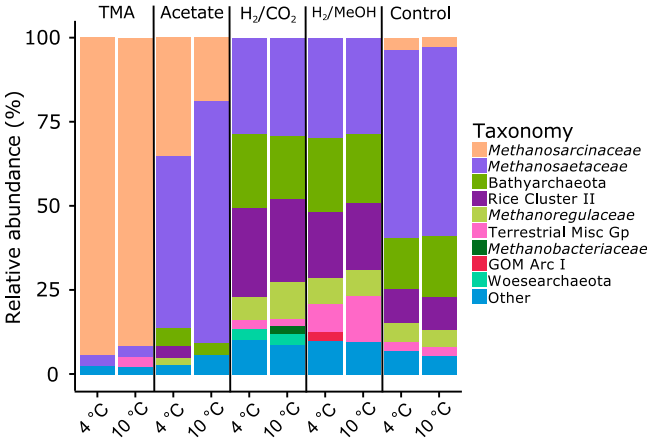

Fig. 3. Phylogenetic classification of amplified archaeal 16S rRNA genes in the methanogenic incubations. The maximum taxonomy depth is on family level. Taxonomic groups with < 2% abundance are grouped in 'Other'.

Discussion

In this study, organic-rich sediment cores were taken from two freshwater thermokarst lakes in Utqiaġvik, Alaska. The respective microbial communities were investigated by 16S rRNA gene amplicon sequencing. The bacterial and archaeal community was very diverse. The sediment cores had a relatively rare bacterial biosphere where 50% of the reads was affiliated to groups with an individual abundance of less than 2%. This high bacterial diversity was not observed in previously described thaw ponds/freshwater sediments (Liebner *et al*., 2008; Rossi *et al*., 2013; Crevecoeur *et al*., 2015; Wang *et al*., 2016; Wagner *et al*., 2017). The dominant members of the bacterial community were Bacteriodetes (16%–19%) similar to a study of polygonal tundra in the Lena Delta, Siberia, where Bacteroidetes constituted almost 50% of the soil microbial community (Liebner *et al*., 2008). Most studies of permafrost thaw ponds that used different DNA extraction and amplification methods, however, have found Proteobacteria to be the most dominant Bacteria (Rossi *et al*., 2013; Crevecoeur *et al*., 2015; Wang *et al*., 2016; Wagner *et al*., 2017), a pattern that was also shown by Wagner *et al*. (2017) who used the same extraction method and 16S rRNA gene amplification as our study. The most abundant Archaea belonged to Rice Cluster II, *Methanosaetaceae*, and Bathyarchaeota, which are commonly found in permafrost sediments and soils (Mondav *et al*., 2017; Winkel *et al*., 2018).

With thaw, previously frozen organic matter will become available for degradation; however, it is impossible to predict what will become available when and in which concentrations. To investigate the microbial response to warming and nutrient availability on the CH_4

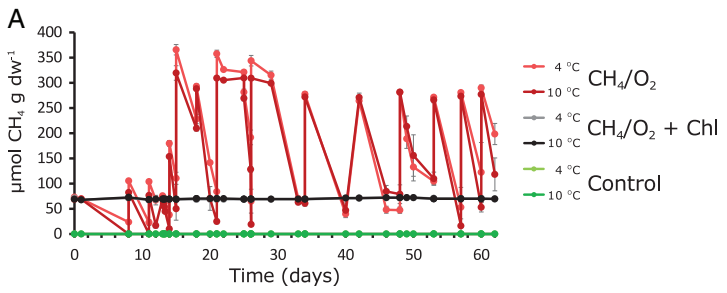

Fig. 4. Oxidation of CH_4 by aerobic methanotrophs in batch incubations with thermokarst lake sediment slurry at 4°C and 10°C. Each data point represents the average from triplicate incubations with methane (CH_4) and oxygen (O_2), biotic control with only O_2 and abiotic control with chloroform (Chl). Error bars indicate standard deviation of the mean. When there was no activity observed, horizontal lines, oxygen was depleted.

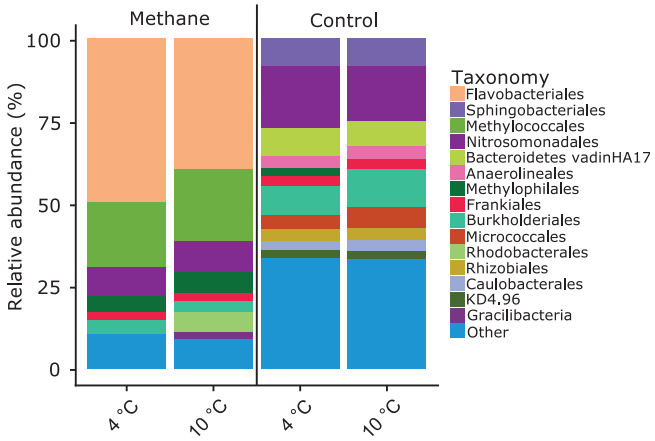

Fig. 5. Phylogenetic classification of amplified bacterial 16S rRNA genes in the aerobic methanotrophic cultures with methane (Methane) or without methane (Control) after 62 days of incubation at 4°C and 10°C. The maximum taxonomy depth is on family level. Taxonomic groups with < 2% abundance are grouped in 'Other'.

emissions, the activity of methanogens and methanotrophs were studied in batch incubations. Here we provided substrate concentrations that were lower than previous studies have used (Allan et al., 2014: 30 mM acetate; Wagner *et al*., 2017: 20 mM trimethylamine (TMA)), and are therefore closer to environmentally relevant conditions. Highest methanogenic activity was observed with TMA (6.6 and 8.5 μmol CH_4 gdw^{-1} d^{-1} at 4°C and 10°C respectively). 50% of the TMA was converted to CH_4. The methanogenic community was clearly enriched in *Methanosarcinaceae*, which was expected based on their substrate spectrum (Garrity *et al*., 2004). Acetoclastic methanogenesis was the second most active process (3.4 and 4.7 μmol CH_4 gdw^{-1} d^{-1} at 4°C and 10°C respectively). About 73% of the acetate was converted to CH_4. Here, *Methanosaetaceae* had a highest relative abundance followed by *Methanosarcinaceae*, which is expected based on their substrate spectrum (Garrity *et al*., 2004). These CH_4 production rates were higher than those found by Allan *et al*. (2014), who observed an average CH_4 flux of 1.8 nmol (g wet weight)$^{-1}$ d^{-1} at 4°C and 0.9 nmol (g wet weight)$^{-1}$ d^{-1} at 22°C in Siberian permafrost microcosms amended with 30 mM acetate during 40–50 days. Although the incubation period in this study was longer, higher rates were also observed after 40 days (0.1 ± 0.02 and 0.2 ± 0.02 μmol CH_4 gdw^{-1} d^{-1} at 4°C and 10°C). The difference in rates is probably mainly caused by the high organic matter content of the Alaskan lake sediments used in this study (25–35 wt%) compared with the Siberian permafrost land soils studied by Allan *et al*. (2014) (4–6 wt%). In the active methanogenic incubations, there was a high temperature sensitivity for TMA and acetate after 98 days (Q_{10} value of 9.8 and 4.2 respectively). High Q_{10} values for methane production in lake sediments were observed before for short incubations (<50 days) (Duc *et al*., 2010; Sepulveda-Jauregui *et al*., 2018). However, the Q_{10} values in our incubations decreased after 279 days to 0.9 and 1.1 for TMA and acetate respectively. At this point, warming did no longer cause significant differences (two-sided *t*-test; $p > 0.05$) to the total CH_4 produced with the two different

Table 3. Quantification of archaeal and bacterial 16S rRNA gene copy number per grams dry weight in the aerobic methanotrophic incubations with methane and oxygen (O_2) and without methane (control) after 62 days.

	Archaeal 16S rRNA gene copies per gdw		Bacterial 16S rRNA gene copies per gdw		Archaeal reads to control		Bacterial reads to control	
Electron acceptors	4°C	10°C	4°C	10°C	4°C	10°C	4°C	10°C
O_2	1.3×10^7 ($\pm 1.6 \times 10^5$)	1.4×10^7 ($\pm 4.3 \times 10^5$)	1.8×10^8 ($\pm 3.6 \times 10^6$)	2.1×10^8 ($\pm 6.8 \times 10^5$)	3	3	6	7
Control	4.3×10^6 ($\pm 4.7 \times 10^4$)	5.0×10^6 ($\pm 4.0 \times 10^4$)	2.8×10^7 ($\pm 4.2 \times 10^5$)	2.9×10^7 ($\pm 7.0 \times 10^5$)	nd	nd	nd	nd

Numbers between brackets display standard deviation of the mean.

substrates, indicating that over a longer time period (>150 days) temperature has no strong effect on the activity of methylotrophic methanogenesis in the incubation bottles. Hydrogenotrophic methanogens were most strongly influenced by the temperature increase (total CH_4 production increased by 66% at 10°C). However, the stoichiometry of the reaction did not match very well as only 3% (for 4°C) and 5% (for 10°C) of the substrates was converted to CH_4. This is an indication that other microbial processes than methanogenesis may be occurring. The total methane production was more pronounced in the presence of acetate and TMA, corroborated by the shifts from hydrogenotrophic to acetoclastic methanogens at elevated temperatures in other studies (Allan *et al*., 2014; McCalley *et al*., 2014; Coolen and Orsi, 2015). The increase in acetate concentration in a natural system often occurs from the reduction of CO_2 with H_2 to acetate by acetogens, which is followed by acetoclastic methanogenesis (Angel *et al*., 2012). Our results are in contrast with studies that found higher abundances of hydrogenotrophic methanogens in the active layer of permafrost (Barbier *et al*., 2012; Deng *et al*., 2015). In the H_2/CO_2 incubations, no clear shift in community composition was observed. The relative abundance of the hydrogenotrophic orders Methanomicrobiales and Methanocellales were slightly increased compared with their abundance in the original sediment, which is in line with the postulation that '*Candidatus* Methanoflorens stordalenmirensis' of the order Methanocellales might be a key player in the methane positive feedback loop in thawing permafrost (McCalley *et al*., 2014; Mondav *et al*., 2014). The CH_4 production rates in the control incubations (1.0 and 1.7 μmol CH_4 gdw^{-1} d^{-1} at 4°C and 10°C respectively) were similar as previously observed in permafrost soil, where CH_4 production ranged between 0.1 and 0.9 μmol CH_4 (g wet $soil)^{-1}$ d^{-1} after 1 week of incubation at 10°C (Barbier *et al*., 2012), assuming the same wet to dry weight conversion factor of 3 as was measured in our study. Methanol amendment (2 mM) might have had an inhibitory effect at both temperatures, possibly related to toxicity, since the observed methanogenic activity was lower than the control. Similar observations were made in a methanogenic mesocosm study with Arctic sediment amended with methanol (10 mM) (Blake *et al*., 2015). Curiously, standard incubations for meso- and thermophilic methylotrophic methanogenic cultures include similar and even higher concentrations of methanol without any of the potential toxic effects observed in our study (Doerfert *et al*., 2009; Mochimaru *et al*., 2009; Allan *et al*., 2014). Although there was no methanogenic activity observed with H_2/MeOH as substrates, the clade Terrestrial Miscellaneous Group, belonging to the class Thermoplasmata, increased in relative abundance in these cultures. The class Thermoplasmata contains the recently found methanogenic lineage Methanomassiliicoccales (Dridi *et al*., 2012; Iino *et al*., 2013) that use H_2 and methanol or methylamines as substrates for methanogenesis, which were also found in thaw ponds and permafrost affected wetlands (Crevecoeur *et al*., 2015; Yang *et al*., 2017).

The CH_4 produced by the methanogens is commonly oxidized to CO_2 by methanotrophs in the sediment. In this study, oxidation rates increased by 57% at 10°C compared with 4°C, which is in line with previous observations from experiments in serum bottles (Knoblauch *et al*., 2008; Duc *et al*., 2010; He *et al*., 2012; Stackhouse *et al*., 2017). Knoblauch *et al*. (2008) observed highest oxidation rates at 22°C in Siberian permafrost soils and an increase at 10°C compared with 0°C and 6°C, although rates were almost 100-fold different between their two sampling sites. He *et al*. (2012) studied Alaskan Arctic lake sediment, where the oxidation rates ranged between 0.3 and 1.3 μmol CH_4 gdw^{-1} d^{-1} at 4°C (5 days of incubation) and 27.3–29.5 μmol CH_4 gdw^{-1} d^{-1} at 10°C (4 days of incubation). We observed rapid enrichment of the methanotrophic community, at both temperature conditions. Type I methanotrophs, from the family *Methylococcaceae*, increased in relative abundance at both temperatures, while type II methanotrophs were not observed in the incubations. The provided high concentrations of CH_4 might have created a niche for type I methanotrophs. The dominance of type I methanotrophs was also found in the active layer of permafrost from the Lena Delta, Siberia (Wagner *et al*., 2005), lake sediments of Lake Qalluuraq, Alaska (He *et al*., 2012), soils from Ellesmere Island, Canada (Martineau *et al*., 2010), and the active layer of permafrost in the Canadian High Arctic (Yergeau *et al*., 2010). Interestingly, the relative abundance of the potential methylotrophs affiliated with the non-CH_4 utilizing methylotrophs of the order Methylophilales increased in the enrichments. The co-occurrence of gammaproteobacterial methanotrophs and non-CH_4-utilizing methylotrophs have been seen before in batch incubations with lake and Arctic sediments amended with CH_4 (Beck *et al*., 2013; Crevecoeur *et al*., 2015; Hernandez *et al*., 2015; Oshkin *et al*., 2015). The applied high concentrations of CH_4 and long incubation time could have led to high activity of the methane monooxygenase enzyme resulting in MeOH release, enabling cross feeding from methanotrophs to these methylotrophs (Martineau *et al*., 2010; He *et al*., 2012; Kalyuzhnaya *et al*., 2013; Tavormina *et al*., 2017). Stable isotope analysis have shown that carbon from CH_4 does get transferred to Methylophilales (Hutchens *et al*., 2004; Beck *et al*., 2013; Kalyuzhnaya *et al*., 2013), but the exact mechanism is still unknown. The most abundant non-methanotrophic bacterial order was Flavobacteriales. It might be possible that the DNA extraction and 16S rRNA gene amplification is biased toward Flavobacteriales resulting in a high

abundance, however, the co-occurrence of Flavobacteriales with methanotrophs has also been observed in other methanotrophic incubations (Barbier *et al*., 2012; Beck *et al*., 2013; Hernandez *et al*., 2015; Oshkin *et al*., 2015) and in thawing permafrost soils (Coolen and Orsi, 2015). Ho *et al*., (2014) even observed a correlation between methane oxidation and heterotrophic richness. The role of these heterotrophs in the community is still elusive but interactions with methane-oxidizing communities have been found with stable isotope probing (Qiu *et al*., 2009). They are likely feeding on accumulated organic compounds such as organic acids and polymeric substances excreted by methanotrophs and other community members or coming from dead and lysed cells (Wendlandt *et al*., 2010; Kalyuzhnaya *et al*., 2013; Ho *et al*., 2014; Yu and Chistoserdova, 2017). Further work is needed to understand potential cross-feeding processes between methanotrophs, methylotrophs and heterotrophs.

Besides the aerobic oxidation of CH_4 by methanotrophic bacteria, the nitrite- and nitrate-dependent AOM by methanotrophic archaea was studied. These processes are carried out by '*Candidatus* Methylomirabilis oxyfera' (Raghoebarsing *et al*., 2006) and '*Candidatus* Methanoperedens nitroreducens' (Haroon *et al*., 2013). '*Candidatus* Methanoperedens' archaea were present in the original sediment (0.3%–2.1% of archaeal reads), indicating that AOM might be possible. However, no AOM activity was observed in our incubations. In the sampled environment, the NO_3^- concentration in the sediments was low, ranging between 0.8 and 2.4 μM. In submarine permafrost, where ANME were found, higher NO_3^- concentrations were detected (Winkel *et al*., 2018). This indicates that NO_3^- does not play an important role in this ecosystem, and when nitrite and nitrate are present they are probably consumed by heterotrophic denitrifiers rather than by ANME Archaea. Other substrates involved in anaerobic methanotrophy should be tested in future studies to determine if AOM is occurring in the sediments of these lakes.

Altogether our results indicate that with the availability of various substrates and increasing temperature both the CH_4 production and consumption rates increase. The microbial community structure was strongly affected by the provided substrate. At higher temperature, there is a rapid response of the methanotrophic community to counteract the increase of the CH_4 emission from methanogens. These laboratory slurry incubations showed that the microbial community was able to adapt to different environmental conditions after nearly a year of incubation. It is essential to better understand the interaction of methanogens and methanotrophs in this ecosystem under increasing substrate availability and elevated temperature scenarios before predications can be made about *in situ* situations.

Experimental procedures

Site description and sediment sampling

Sediment cores were collected from two nearby thermokarst lakes (Lake Emaiksoun and Unnamed Lake) during a winter field campaign carried out by the Vrije Universiteit Amsterdam in November 2015 to the northernmost US settlement of Utqiaġvik in the North Slope of Alaska, The United States. The two sampled lakes had maximum water depths of about 2.6 m, which made them relatively deep in comparison to the surrounding lakes (Hinkel *et al*., 2012). Despite the low depth, the lake bathymetry fell off steeply within a few meters from the shorelines. Both sampled lakes were located within wider drained lake basins with old remnant shorelines suggesting lake drainage at some point in the past. The sediment cores were collected in duplicates from seven different sites of the frozen lakes surfaces with a hand-operated Uwitec gravity coring system (Supporting Information Table S1, Supporting Information Fig. S1). The cores had a diameter of 9 cm and lengths ranging from 40 to 86 cm. On the day of coring, pore-water samples were obtained from seven cores (one core at each site) at a 10 cm resolution with ceramic rhizons (pore size 0.12–0.18 μm) from Rhizosphere (Wageningen, The Netherlands). Porewater samples were treated with potassium iodide (KI) to prevent microbial activity. The cores were stored horizontally in the dark at 4°C at the Vrije Universiteit Amsterdam, the Netherlands. Pore water data was analyzed by inductive coupled plasma-optical emission spectrometry (ICP-OES) for Al, Ca, Fe, K, Mg, Mn, Na, P, S, Si, Zn (iCap 6300, Thermo Scientific, Waltham, MA) and continuous flow analysis (CFA) for NO_3, NH_4, PO_4, Na, K and Cl (Supporting Information Tables S2 and S3) (Bran+Luebbe Auto Analyzer, SPX Flow, Norderstedt, Germany; Seal Analytical AutoAnalyzer 3, Seal Analytical, Southampton, UK).

Incubation experiments

The incubation experiments were started within half a year of sampling. The elemental data from pore water data analysis was used for medium design. The active top layer sediments from the seven cores (128 g) were mixed 1:10 weight/volume with anaerobic freshwater medium [KH_2PO_2 0.20 g L^{-1}, NH_4Cl 0.25 g L^{-1}, NaCl 1.00 g L^{-1}, $MgCl_2 \cdot 6H_2O$ 0.40 g L^{-1}, KCl 0.50 g L^{-1} and $CaCl_2 \cdot 2H_2O$ 0.15 g L^{-1} in grade 3 demineralized water, 1 ml L^{-1} trace element solution SL-10 (DSMZ) with $CeCl_3 \cdot 7H_2O$ 24 mg L^{-1}, $Na_2SeO_3 \cdot 5H_2O$ 30 mg L^{-1} and $Na_2WO_4 \cdot 2H_2O$ 40 mg L^{-1} and 1 ml L^{-1} vitamin solution (DSMZ) (biotin 20 mg L^{-1}, folic acid 20 mg L^{-1}, pyridoxine HCl 100 mg L^{-1}, thiamine HCl $\cdot 2H_2O$ 5 mg L^{-1}, riboflavin 5 mg L^{-1}, nicotinic acid 5 mg L^{-1}, Ca-P-pantothenate 5 mg L^{-1}, cobalamin 0.10 mg L^{-1}, p-

aminobenzoic acid 5 mg L^{-1} and lipoic acid 5 mg L^{-1})]. The final pH of the slurries was 6.3.

• *Methanogenic incubations.* 50 ml aliquots of the slurry were distributed over 120 ml sterile glass serum bottles. Triplicate incubations for 4°C and 10°C were prepared for acetoclastic, hydrogenotrophic, methylotrophic and hydrogen-dependent methylotrophic methanogens and biotic controls without any substrates. Final concentrations of 2 mM acetate, TMA or MeOH/H_2 were added to the respective incubations. Culture bottles were sealed with airtight red butyl rubber stoppers and secured with open-top aluminium crimp caps. Anaerobic conditions were created by three 15-min cycles of vacuuming and subsequent gassing for three minutes with 1 bar Argon overpressure; in the end the overpressure was removed. For the hydrogenotrophic incubations, H_2 (8 mM) and CO_2 (2 mM) were added to the serum bottles.

To remove trace oxygen, 0.1 ml sterile 150 g L^{-1} L-cysteine and 0.1 ml sterile 150 g L^{-1} Na_2S were added. The serum bottles were incubated in the dark at 4°C and 10°C under continuous shaking at 150 rpm. During incubation, substrates were replenished when needed. For acetate amended cultures, in total 14 mM of acetate was added (pulses of 4 mM at day 64 and 2 mM at day 141, 190, 211 and 234) and 12 mM of TMA (pulses of 2 mM at day 141, 190, 211, 234 and 269) during the incubation period of 279 days. For H_2/CO_2 incubations a total of 56 mM H_2 and 22 mM CO_2 was added (at day 28, 36, 44, 48, 50, 51, 52, 55, 57, and 62) and for H_2/methanol incubations this was 16 mM H_2 and 16 mM methanol (in pulses of 2 mM on day 10, 21, 28, 36, 44, 141, and 255). All concentrations were calculated based on 50 ml liquid volume, assuming all of the substrate dissolves over time.

Due to high substrate consumption in the H_2/CO_2 incubations, biomass was harvested after 64 days. All other enrichment cultures were terminated after 279 days. The pH was measured at the end of the incubation period (Metrohm, Herisau, Switzerland; Hanna Instruments, Betuwehaven, The Netherlands). Contents from triplicate individual bottles were pooled and centrifuged for 10 min at 2800× rcf (Eppendorf, Nijmegen, The Netherlands). Pellets were stored at −18°C until further analysis.

• *Aerobic methanotrophic incubations.* 50 ml slurry was transferred to 120 ml culture bottles and 2 mM of CH_4 (final concentration for 50 ml) was added to the headspace. The biotic control contained only the sediment slurry; the abiotic control contained CH_4 and 500 μM chloroform to inhibit general microbial activity. Triplicate serum bottles were incubated in the dark at 4°C and 10°C under continuous shaking at 150 rpm. After near complete oxidation of CH_4 or stagnation of methanotrophic activity, bottles were flushed with three times the headspace volume with 0.2 μM filter sterilized air before addition of CH_4. Due to high activity, CH_4 concentrations were increased to 7.8 mM after 2 weeks of incubations (1:1.5 CH_4:O_2). Cultures were harvested after 62 days, using the same method as described above.

• *Anaerobic methanotroph incubations.* About 50 ml of slurry was amended with 0.25 mM nitrite (NO_2^-) or 2 mM nitrate (NO_3^-) together with 1 mM $^{13}CH_4$ in 120 ml culture bottles. Control incubations were prepared either without electron acceptors or $^{13}CH_4$. Bottles were capped and gassed/degassed as described in the aerobic methanotrophic incubations; a final overpressure of 0.5 bar Argon was applied. Thereafter, $^{13}CH_4$ was added. The triplicate serum bottles were incubated in the dark at 4°C and 10°C under continuous shaking at 150 rpm. After 125 days, 14 ml of $^{13}CH_4$ (20% of headspace) was added to stimulate activity. After 246 days, the pH (Hanna Instruments, Betuwehaven, The Netherlands) and concentration of NO_2^- and NO_3^- (Griess, 1879) were measured by taking an aliquot of the culture, when depleted NO_2^- and NO_3^- were added. After, concentrations of NO_2^- and NO_3^- were monitored twice a month and were replenished when they dropped below 20 μM for NO_2^- and 0.8 mM for NO_3^-. Headspace $^{13}CO_2$ was monitored for 450 days.

Analysis of substrates and products

Gas samples (50 μl) were withdrawn with a gas-tight glass syringe (Hamilton, Reno, NE) and injected into a HP 5890 gas chromatograph (Hewlett Packard, Palo Alto, CA) equipped with a Porapaq Q 100/120 mesh (Sigma Aldrich, Saint Louis, MI) and a flame ionization detector (FID) for CH_4 detection and a thermal conductivity detector (TCD) for measuring H_2, CH_4 and CO_2 simultaneously using N_2 as carrier gas. An Agilent 6890 series gas chromatograph coupled to a mass spectrometer (Agilent, Santa Clara, CA) equipped with a Porapak Q column heated at 80°C with Helium as the carrier gas was used for measurements of CO_2 and O_2. Concentration of gases in the incubations was calculated by the sum of the gas concentration in the headspace and liquid phase divided by the slurry dry weight. Maximum production and consumption rates of CH_4 were calculated by subtracting each measure point by previous time point and divide it by days and grams of dry weight of 50 ml slurry. The Q10 coefficient was calculated as described in Sepulveda-Jaurequi *et al*. (2018). The maximum Q10 was determined by the comparison of the rates occurring at the same time point. The final Q10 was determined by using the final measurement. Two-sided *t*-tests were performed in Microsoft Office Excel (2016).

Nitrate concentrations in the cultures were estimated with Merckoquant test strips (0–80 mg L^{-1}, Merck, Germany), nitrite was measured using the nitrite determination protocol by Griess (1879).

Molecular analysis

- *DNA isolation.* Sediment samples were taken aseptically from the original sediments and stored at −18°C until DNA isolation. Samples from batch incubation cultures were pelleted by centrifugation for 10 min at 20,000*g* (Eppendorf, Nijmegen, The Netherlands). Samples for DNA analysis were obtained by pooling equal amounts of pelleted slurry sample per triplicate bottle. DNA was extracted in duplicate per sample using the PowerSoil DNA Isolation Kit (MO BIO, Qiagen, Venlo, The Netherlands) following the manufacturer's instructions with the following modifications: the initial PowerBead Tube vortex step was carried out using a bead beater at 30 bps for 10 min. The primary centrifugation step was done for 1 min at 10,000*g.* DNA elution was performed with 2 × 25 μl sterile Milli-Q with 2 min incubation at room temperature prior to centrifugation. The second elution centrifugation step was carried out for 1 min at 10,000*g.* DNA quality was checked by agarose gel electrophoresis, spectrophotometrically using the NanoDrop 1000 (Invitrogen, Thermo Fisher, Carlsbad, CA) and fluorometrically using the Qubit dsDNA HS Assay Kit (Invitrogen, Thermo Fisher, Carlsbad, CA) according to the manufacturer's instructions. Duplicate samples with highest yield and quality were selected for downstream applications.

- *Phylogenetic analysis.* To assess the diversity of Bacteria and Archaea, 16S rRNA gene amplicon sequencing was performed on an Illuminia Miseq Next Generation Sequencing by Macrogen, Korea. The primers for bacterial amplification were Bac341F (5′-CCTACGGGNGGCWGCAG-3′) (Herlemann *et al*., 2011) and Bac806R (5′-GGACTACHVGGGTWTCTAAT-3′) (Caporaso *et al*., 2012). For archaeal amplification the primers were Arch349F (5′-GYGCASCAGKCGMGAAW-3′) (Takai and Horikoshi, 2000) and Arch806R (5′-GGACTACVSGGGTATCTAAT-3′) (Takai and Horikoshi, 2000). For the output data, 90% of the reads had a Q20 quality score of 90% (Q30 for ≥ 81% of reads) or higher and average total read count was 161,000 reads per sample. Sequences were filtered for a length between 400 and 500 base pairs (bp). For additional analyses with single-end reads minimum read length was set to 291 bp. Amplicon sequences were quality checked for chimeras using the UCHIME algorithm (Edgar *et al*., 2011), clustered into OTUs with a 97% identity cut-off value and classified using the SILVA v128 16S rRNA gene non-redundant database (SSURef_NR99_128_SILVA) and the Bayesian classifier ('wang') using the MySeq SOP (http://www.mothur.org/) (Schloss *et al*., 2009). 'Chloroplasts', 'Mitochondria', 'unknown' and 'Eukaryota' were removed for both datasets, 'Bacteria' and 'Archaea' were removed for the archaeal and bacterial sequence datasets respectively. The 'filename.taxonomy' and 'filename.shared' files were used for downstream analyses with R (https://www.r-project.org/) (R Development Core Team, 2013) and Rstudio v3 (https://www.rstudio.com/) (RStudio Team, 2015) as described in in 't Zandt *et al*. (2017). Singletons were removed and data was rarefied in R (see rarefraction curves in Supporting Information Figs. S6–S9). All sequencing data were submitted to the GenBank databases under the BioProject SRP133831.

  Diversity indices were calculated on the OTU tables with the summary.single command in mothur using 'chao' to assess community richness; 'simpsoneven' and 'shannoneven' to assess community evenness and 'simpson' and 'shannon' to assess community diversity. NMDS plots were made using the OTU output tables from mothur. All data was analyzed using r (https://www.r-project.org/) (R Development Core Team, 2013) and Rstudio v3 (https://www.rstudio.com/) (RStudio Team, 2015). All OTUs with 1 hit or less per sample were removed to reduce noise. Plots were made using the 'metaMDS' tool from the 'Vegan' package in R (Oksanen *et al*., 2018), stress was calculated using 20 iterations. Colour labels were added with 'rgl' (Adler *et al*., 2018).

- *Cloning, sequencing and qPCR.* 16S rRNA gene copy numbers in the environmental samples and enrichment samples were quantified with the archaeal and bacterial Illumina primers described above. Quality and size checks were performed using agarose gel electrophoresis. All qPCR reactions were performed using PerfeCTA Quanta master mix (Quanta Bio, Beverly, MA) and 96-well optical PCR plates (Bio-Rad Laboratories B.V., Veenendaal, The Netherlands) with optical adhesive covers (Applied Biosystems, Foster City, CA). All reactions were performed on a C1000 Touch thermal cycler equipped with a CFX96 Touch™ Real-Time PCR Detection System (Bio-Rad Laboratories B.V., Veenendaal, The Netherlands); 0.5 ng DNA template was used per reaction. Negative controls were added to each run by replacing the template with sterile Milli-Q water. Standard curves were constructed with a 10-fold serial dilution of a quantified copy number of pGEM®-T Easy plasmids with inserted Illumina PCR fragments of archaeal and bacterial 16S rRNA gene (Promega, Madison, WI). All qPCR data was analyzed using the Bio-Rad CFX Manager version 3.0 (Bio-Rad Laboratories B.V., Veenendaal, The Netherlands).

Acknowledgements

We thank Jeroen Frank for the great discussions about sequencing analysis, Sebastian Krosse for pore-water data analysis, and Han Dolman for fruitful discussions and input. This research was supported by the Netherlands Organization for Scientific

Research through the Netherlands Earth System Science Center (NESSC) Gravitation Grant [grant number 024.002.001 to MitZ, AdJ, OR, JD, OM and MJ], the Soehngen Institute of Anaerobic Microbiology (SIAM) Gravitation Grant [grant number 024.002.002 to MJ and CW] and the European Research Council Advanced Grant [grant number 339880 to MJ].

References

Abbott, B. W., Jones, J. B., Godsey, S. E., Larouche, J. R., and Bowden, W. B. (2015) Patterns and persistence of hydrologic carbon and nutrient export from collapsing upland permafrost. *Biogeosciences* **12**: 3725–3740.

Adler, D., Murdoch, D., Nenadic, O., Urbanek, S., Chen, M., Gebhardt, A., et al. (2018) RGL - 3D visualization device system for R using OpenGL. https://r-forge.r-project.org/projects/rgl/

Allan, J., Ronholm, J., Mykytczuk, N. C. S., Greer, C. W., Onstott, T. C., and Whyte, L. G. (2014) Methanogen community composition and rates of methane consumption in Canadian High Arctic permafrost soils. *Environ Microbiol Rep* **6**: 136–144.

Angel, R., Claus, P., and Conrad, R. (2012) Methanogenic archaea are globally ubiquitous in aerated soils and become active under wet anoxic conditions. *ISME J* **6**: 847–862.

Barbier, B. A., Dziduch, I., Liebner, S., Ganzert, L., Lantuit, H., Pollard, W., and Wagner, D. (2012) Methane-cycling communities in a permafrost-affected soil on Herschel Island, Western Canadian Arctic: active layer profiling of *mcrA* and *pmoA* genes. *FEMS Microbiol Ecol* **82**: 287–302.

Basiliko, N., Yavitt, J. B., Dees, P. M., and Merkel, S. M. (2003) Methane biogeochemistry and methanogen communities in two Northern peatland ecosystems, New York State. *Geomicrobiol J* **20**: 563–577.

Beck, D. A. C., Kalyuzhnaya, M. G., Malfatti, S., Tringe, S. G., Glavina del Rio, T., Ivanova, N., *et al*. (2013) A metagenomic insight into freshwater methane-utilizing communities and evidence for cooperation between the *Methylococcaceae* and the *Methylophilaceae*. *PeerJ* **1**: e23.

Black, R.F. (1964) *Gubik Formation of Quaternary Age in Northern Alaska.* Washington: United States Government Printing Office.

Blake, L. I., Tveit, A., Øvreås, L., Head, I. M., and Gray, N. D. (2015) Response of methanogens in Arctic sediments to temperature and methanogenic substrate availability. *PLoS One* **10**: e0129733.

Caporaso, J. G., Lauber, C. L., Walters, W. A., Berg-Lyons, D., Huntley, J., Fierer, N., *et al*. (2012) Ultra-high-throughput microbial community analysis on the Illumina HiSeq and MiSeq platforms. *ISME J* **6**: 1621–1624.

Cheng, L., Qiu, T.-L., Yin, X.-B., Wu, X.-L., Hu, G.-Q., Deng, Y., and Zhang, H. (2007) *Methermicoccus shengliensis* gen. nov., sp. nov., a thermophilic, methylotrophic methanogen isolated from oil-production water, and proposal of *Methermicoccaceae* fam. nov. *Int J Syst Evol Microbiol* **57**: 2964–2969.

Coolen, M. J. L., and Orsi, W. D. (2015) The transcriptional response of microbial communities in thawing Alaskan permafrost soils. *Front Microbiol* **6**: 197.

Crevecoeur, S., Vincent, W. F., Comte, J., and Lovejoy, C. (2015) Bacterial community structure across environmental gradients in permafrost thaw ponds: methanotroph-rich ecosystems. *Front Microbiol* **6**: 192.

Dan, D., Zhang, D.-P., Liu, W.-C., Lu, C.-G., and Zhang, T.-T. (2014) Diversity analysis of bacterial community from permafrost soil of Mo-he in China. *Indian J Microbiol* **54**: 111–113.

Dean, J. F., Middelburg, J. J., Röckmann, T., Aerts, R., Blauw, L. G., Egger, M., *et al*. (2018) Methane feedbacks to the global climate system in a warmer world. *Rev Geophys* **56**: 1–44.

Deng, J., Gu, Y., Zhang, J., Xue, K., Qin, Y., Yuan, M., *et al*. (2015) Shifts of tundra bacterial and archaeal communities along a permafrost thaw gradient in Alaska. *Mol Ecol* **24**: 222–234.

Dibike, Y., Prowse, T., Saloranta, T., and Ahmed, R. (2011) Response of Northern Hemisphere lake-ice cover and lake-water thermal structure patterns to a changing climate. *Hydrol Process* **25**: 2942–2953.

Doerfert, S. N., Reichlen, M., Iyer, P., Wang, M., and Ferry, J. G. (2009) *Methanolobus zinderi* sp. nov., a methylotrophic methanogen isolated from a deep subsurface coal seam. *Int J Syst Evol Microbiol* **59**: 1064–1069.

Dridi, B., Fardeau, M. L., Ollivier, B., Raoult, D., and Drancourt, M. (2012) *Methanomassiliicoccus luminyensis* gen. nov., sp. nov., a methanogenic archaeon isolated from human faeces. *Int J Syst Evol Microbiol* **62**: 1902–1907.

Duc, N. T., Crill, P., and Bastviken, D. (2010) Implications of temperature and sediment characteristics on methane formation and oxidation in lake sediments. *Biogeochemistry* **100**: 185–196.

Edgar, R. C., Haas, B. J., Clemente, J. C., Quince, C., and Knight, R. (2011) UCHIME improves sensitivity and speed of chimera detection. *Bioinformatics* **27**: 2194–2200.

Frey, B., Rime, T., Phillips, M., Stierli, B., Hajdas, I., Widmer, F., and Hartmann, M. (2016) Microbial diversity in European alpine permafrost and active layers. *FEMS Microbiol Ecol* **92**: fiw018.

Galand, P. E., Fritze, H., Conrad, R., and Yrjälä, K. (2005) Pathways for methanogenesis and diversity of methanogenic archaea in three boreal peatland ecosystems. *Appl Environ Microbiol* **71**: 2195–2198.

Ganzert, L., Bajerski, F., and Wagner, D. (2014) Bacterial community composition and diversity of five different permafrost-affected soils of Northeast Greenland. *FEMS Microbiol Ecol* **89**: 426–441.

Garrity, G. M., Bell, J. A., and Lilburn, T. G. (2004) Taxonomic outline of the prokaryotes . In *Bergey's Manual of Systematic Bacteriology*. Bergey, D. H., Buchanan, R. E., and Gibbons, N. E. (eds). Baltimore: Williams & Wilkins.

Gill, A. L., Giasson, M.-A., Yu, R., and Finzi, A. C. (2017) Deep peat warming increases surface methane and carbon dioxide emissions in a black spruce-dominated ombrotrophic bog. *Glob Chang Biol* **23**: 5398–5411.

Griess, P. (1879) Bemerkungen zu der Abhandlung der HH. Weselsky und Benedikt "Ueber einige Azoverbindungen". *Berichte der Dtsch Chem Gesellschaft* **12**: 426–428.

Grosse, G., Jones, B., and Arp, C. (2013) Thermokarst lakes, drainage, and drained basins . In *Treatise on Geomorphology*, Shroder, J., Giardino, R., and Harbor, J. (eds). San Diego, CA: Academic Press, pp. 325–353.

Hansen, A. A., Herbert, R. A., Mikkelsen, K., Jensen, L. L., Kristoffersen, T., Tiedje, J. M., *et al*. (2007) Viability, diversity and composition of the bacterial community in a high Arctic permafrost soil from Spitsbergen, Northern Norway. *Environ Microbiol* **9**: 2870–2884.

Haroon, M. F., Hu, S., Shi, Y., Imelfort, M., Keller, J., Hugenholtz, P., *et al*. (2013) Anaerobic oxidation of methane coupled to nitrate reduction in a novel archaeal lineage. *Nature* **500**: 567–570.

He, R., Wooller, M. J., Pohlman, J. W., Quensen, J., Tiedje, J. M., and Leigh, M. B. (2012) Shifts in identity and activity of methanotrophs in Arctic lake sediments in response to temperature changes. *Appl Environ Microbiol* **78**: 4715–4723.

Herlemann, D. P., Labrenz, M., Jürgens, K., Bertilsson, S., Waniek, J. J., and Andersson, A. F. (2011) Transitions in bacterial communities along the 2000 km salinity gradient of the Baltic Sea. *ISME J* **5**: 1571–1579.

Hernandez, M. E., Beck, D. A. C., Lidstrom, M. E., and Chistoserdova, L. (2015) Oxygen availability is a major factor in determining the composition of microbial communities involved in methane oxidation. *PeerJ* **3**: e801.

Hinkel, K. M., Sheng, Y., Lenters, J. D., Lyons, E. A., Beck, R. A., Eisner, W. R., and Wang, J. (2012) Thermokarst lakes on the Arctic coastal plain of Alaska: geomorphic controls on bathymetry. *Permafr Periglac Process* **23**: 218–230.

Ho, A., de Roy, K., Thas, O., De Neve, J., Hoefman, S., Vandamme, P., *et al*. (2014) The more, the merrier: heterotroph richness stimulates methanotrophic activity. *ISME J* **8**: 1945–1948.

Høj, L., Olsen, R. A., and Torsvik, V. L. (2008) Effects of temperature on the diversity and community structure of known methanogenic groups and other archaea in High Arctic peat. *ISME J* **2**: 37–48.

Hugerth, L. W., Wefer, H. A., Lundin, S., Jakobsson, H. E., Lindberg, M., Rodin, S., *et al*. (2014) DegePrime, a program for degenerate primer design for broad-taxonomic-range PCR in microbial ecology studies. *Appl Environ Microbiol* **80**: 5116–5123.

Hutchens, E., Radajewski, S., Dumont, M. G., McDonald, I. R., and Murrell, J. C. (2004) Analysis of methanotrophic bacteria in Movile Cave by stable isotope probing. *Environ Microbiol* **6**: 111–120.

Iino, T., Tamaki, H., Tamazawa, S., Ueno, Y., Ohkuma, M., Suzuki, K.-I., *et al*. (2013) "*Candidatus* Methanogranum caenicola": a novel methanogen from the anaerobic digested sludge, and proposal of *Methanomassiliicoccaceae* fam. nov. and *Methanomassiliicoccales* ord. nov., for a methanogenic lineage of the class Thermopl. *Microbes Environ* **28**: 244–250.

Kalyuzhnaya, M. G., Yang, S., Rozova, O. N., Smalley, N. E., Clubb, J., Lamb, A., *et al*. (2013) Highly efficient methane biocatalysis revealed in a methanotrophic bacterium. *Nat Commun* **4**: 2785.

Karlsson, J. M., Jaramillo, F., and Destouni, G. (2015) Hydro-climatic and lake change patterns in Arctic permafrost and non-permafrost areas. *J Hydrol* **529**: 134–145.

Kirschke, S., Bousquet, P., Ciais, P., Saunois, M., Canadell, J. G., Dlugokencky, E. J., *et al*. (2013) Three decades of global methane sources and sinks. *Nat Geosci* **6**: 813–823.

Knoblauch, C., Zimmermann, U., Blumenberg, M., Michaelis, W., and Pfeiffer, E.-M. (2008) Methane turnover and temperature response of methane-oxidizing bacteria in permafrost-affected soils of northeast Siberia. *Soil Biol Biochem* **40**: 3004–3013.

Koch, J. C., Gurney, K., and Wipfli, M. S. (2014) Morphology-dependent water budgets and nutrient fluxes in Arctic thaw ponds. *Permafr Periglac Process* **25**: 79–93.

Kotsyurbenko, O. R. (2005) Trophic interactions in the methanogenic microbial community of low-temperature terrestrial ecosystems. *FEMS Microbiol Ecol* **53**: 3–13.

Kotsyurbenko, O. R., Friedrich, M. W., Simankova, M. V., Nozhevnikova, A. N., Golyshin, P. N., Timmis, K. N., and Conrad, R. (2007) Shift from acetoclastic to H_2-dependent methanogenesis in a West Siberian peat bog at low pH values and isolation of an acidophilic *Methanobacterium* strain. *Appl Environ Microbiol* **73**: 2344–2348.

Kotsyurbenko, O. R., Glagolev, M. V., Nozhevnikova, A. N., and Conrad, R. (2001) Competition between homoacetogenic bacteria and methanogenic archaea for hydrogen at low temperature. *FEMS Microbiol Ecol* **38**: 153–159.

Liebner, S., Ganzert, L., Kiss, A., Yang, S., Wagner, D., and Svenning, M. M. (2015) Shifts in methanogenic community composition and methane fluxes along the degradation of discontinuous permafrost. *Front Microbiol* **6**: 356.

Liebner, S., Harder, J., and Wagner, D. (2008) Bacterial diversity and community structure in polygonal tundra soils from Samoylov Island, Lena Delta, Siberia. *Int Microbiol* **11**: 195–202.

Liebner, S., Rublack, K., Stuehrmann, T., and Wagner, D. (2009) Diversity of aerobic methanotrophic bacteria in a permafrost active layer soil of the Lena Delta, Siberia. *Microb Ecol* **57**: 25–35.

Liebner, S., and Wagner, D. (2007) Abundance, distribution and potential activity of methane oxidizing bacteria in permafrost soils from the Lena Delta, Siberia. *Environ Microbiol* **9**: 107–117.

Martineau, C., Whyte, L. G., and Greer, C. W. (2010) Stable isotope probing analysis of the diversity and activity of methanotrophic bacteria in soils from the Canadian High Arctic. *Appl Environ Microbiol* **76**: 5773–5784.

Martinez-Cruz, K., Leewis, M.-C., Herriott, I. C., Sepulveda-Jauregui, A., Anthony, K. W., Thalasso, F., and Leigh, M. B. (2017) Anaerobic oxidation of methane by aerobic methanotrophs in sub-Arctic lake sediments. *Sci Total Environ* **607–608**: 23–31.

Mayumi, D., Mochimaru, H., Tamaki, H., Yamamoto, K., Yoshioka, H., Suzuki, Y., *et al*. (2016) Methane production from coal by a single methanogen. *Science (80-)* **354**: 222–225.

McCalley, C. K., Woodcroft, B. J., Hodgkins, S. B., Wehr, R. A., Kim, E.-H., Mondav, R., *et al*. (2014) Methane dynamics regulated by microbial community response to permafrost thaw. *Nature* **514**: 478–481.

Metje, M., and Frenzel, P. (2007) Methanogenesis and methanogenic pathways in a peat from subarctic permafrost. *Environ Microbiol* **9**: 954–964.

Mochimaru, H., Tamaki, H., Hanada, S., Imachi, H., Nakamura, K., Sakata, S., and Kamagata, Y. (2009) *Methanolobus profundi* sp. nov., a methylotrophic methanogen isolated from deep subsurface sediments in a natural gas field. *Int J Syst Evol Microbiol* **59**: 714–718.

Mondav, R., McCalley, C. K., Hodgkins, S. B., Frolking, S., Saleska, S. R., Rich, V. I., *et al*. (2017) Microbial network, phylogenetic diversity and community membership in the active layer across a permafrost thaw gradient. *Environ Microbiol* **19**: 3201–3218.

Mondav, R., Woodcroft, B. J., Kim, E.-H., McCalley, C. K., Hodgkins, S. B., Crill, P. M., *et al*. (2014) Discovery of a novel methanogen prevalent in thawing permafrost. *Nat Commun* **5**: 3212.

Myhre, G., Shindell, D., Bréon, F.-M., Collins, W., Fuglestvedt, J., Huang, J., *et al*. (2013) Anthropogenic and natural radiative forcing. In *Climate Change 2013: The Physical Science Basis. Contribution of Working Group I to the Fifth Assessment Report of the Intergovernmental Panel on Climate Change*, Stocker, T., Qin, D., Plattner, G., Tignor, M., Allen, S., Boschung, J., *et al*. (eds). Cambridge, United Kingdom and New York, NY: Cambridge University Press, pp. 659–740.

Narancic, B., Wolfe, B. B., Pienitz, R., Meyer, H., and Lamhonwah, D. (2017) Landscape-gradient assessment of thermokarst lake hydrology using water isotope tracers. *J Hydrol* **545**: 327–338.

Nozhevnikova, A. N., Zepp, K., Vazquez, F., Zehnder, A. J. B., and Holliger, C. (2003) Evidence for the existence of psychrophilic methanogenic communities in anoxic sediments of deep lakes. *Appl Environ Microbiol* **69**: 1832–1835.

Oksanen, J., Blanchet, F.G., Friendly, M., Kindt, R., Legendre, P., McGlinn, D., et al. (2018) *Vegan: Community Ecology Package*. R package version 2.3-3. https://cran.r-project.org/web/packages/vegan/index.html

Olefeldt, D., Goswami, S., Grosse, G., Hayes, D., Hugelius, G., Kuhry, P., *et al*. (2016) Circumpolar distribution and carbon storage of thermokarst landscapes. *Nat Commun* **7**: 13043.

Oshkin, I. Y., Beck, D. A., Lamb, A. E., Tchesnokova, V., Benuska, G., McTaggart, T. L., *et al*. (2015) Methane-fed microbial microcosms show differential community dynamics and pinpoint taxa involved in communal response. *ISME J* **9**: 1119–1129.

Osterkamp, T. E., Jorgenson, M. T., Schuur, E. A. G., Shur, Y. L., Kanevskiy, M. Z., Vogel, J. G., and Tumskoy, V. E. (2009) Physical and ecological changes associated with warming permafrost and thermokarst in Interior Alaska. *Permafr Periglac Process* **20**: 235–256.

Overduin, P. P., Liebner, S., Knoblauch, C., Günther, F., Wetterich, S., Schirrmeister, L., *et al*. (2015) Methane oxidation following submarine permafrost degradation: measurements from a central Laptev Sea shelf borehole. *J Geophys Res Biogeosci* **120**: 965–978.

Prowse, T., Alfredsen, K., Beltaos, S., Bonsal, B., Duguay, C., Korhola, A., *et al*. (2011) Past and future changes in Arctic lake and river ice. *Ambio* **40**: 53–62.

Qiu, Q., Conrad, R., and Lu, Y. (2009) Cross-feeding of methane carbon among bacteria on rice roots revealed by DNA-stable isotope probing. *Environ Microbiol Rep* **1**: 355–361.

R Development Core Team. (2013) *R: A Language and Environment for Statistical Computing*. Vienna, Austria: The R Foundation for Statistical Computing.

Raghoebarsing, A. A., Pol, A., van de Pas-Schoonen, K. T., Smolders, A. J. P., Ettwig, K. F., Rijpstra, W. I. C., *et al*. (2006) A microbial consortium couples anaerobic methane oxidation to denitrification. *Nature* **440**: 918–921.

Rossi, P. G., Laurion, I., and Lovejoy, C. (2013) Distribution and identity of Bacteria in subarctic permafrost thaw ponds. *Aquat Microb Ecol* **69**: 231–245.

RStudio Team (2015) Rstudio: Integrated Development for R. Boston, MA: RStudio, Inc.

Schloss, P. D., Westcott, S. L., Ryabin, T., Hall, J. R., Hartmann, M., Hollister, E. B., *et al*. (2009) Introducing mothur: open-source, platform-independent, community-supported software for describing and comparing microbial communities. *Appl Environ Microbiol* **75**: 7537–7541.

Schuur, E. A. G., McGuire, A. D., Schädel, C., Grosse, G., Harden, J. W., Hayes, D. J., *et al*. (2015) Climate change and the permafrost carbon feedback. *Nature* **520**: 171–179.

Semrau, J. D., DiSpirito, A. A., and Yoon, S. (2010) Methanotrophs and copper. *FEMS Microbiol Rev* **34**: 496–531.

Sepulveda-Jauregui, A., Hoyos-Santillan, J., Martinez-Cruz, K., Walter Anthony, K. M., Casper, P., Belmonte-Izquierdo, Y., and Thalasso, F. (2018) Eutrophication exacerbates the impact of climate warming on lake methane emission. *Sci Total Environ* **636**: 411–419.

Stackhouse, B., Lau, M. C. Y., Vishnivetskaya, T., Burton, N., Wang, R., Southworth, A., *et al*. (2017) Atmospheric CH_4 oxidation by Arctic permafrost and mineral cryosols as a function of water saturation and temperature. *Geobiology* **15**: 94–111.

Takai, K., and Horikoshi, K. (2000) Rapid detection and quantification of members of the archaeal community by quantitative PCR using fluorogenic probes. *Appl Environ Microbiol* **66**: 5066–5072.

Tavormina, P. L., Kellermann, M. Y., Antony, C. P., Tocheva, E. I., Dalleska, N. F., Jensen, A. J., *et al*. (2017) Starvation and recovery in the deep-sea methanotroph *Methyloprofundus sedimenti*. *Mol Microbiol* **103**: 242–252.

Thauer, R. K., and Shima, S. (2008) Methane as fuel for anaerobic microorganisms. *Ann N Y Acad Sci* **1125**: 158–170.

Trotsenko, Y. A., and Khmelenina, V. N. (2005) Aerobic methanotrophic bacteria of cold ecosystems. *FEMS Microbiol Ecol* **53**: 15–26.

Trotsenko, Y. A., and Murrell, J. C. (2008) Metabolic aspects of aerobic oligate methanotrophy. *Adv Appl Microbiol* **63**: 183–229.

Voigt, C., Lamprecht, R. E., Marushchak, M. E., Lind, S. E., Novakovskiy, A., Aurela, M., *et al*. (2017) Warming of subarctic tundra increases emissions of all three important greenhouse gases - carbon dioxide, methane, and nitrous oxide. *Glob Chang Biol* **23**: 3121–3138.

Wagner, D., Lipski, A., Embacher, A., and Gattinger, A. (2005) Methane fluxes in permafrost habitats of the Lena Delta: effects of microbial community structure and organic matter quality. *Environ Microbiol* **7**: 1582–1592.

Wagner, R., Zona, D., Oechel, W., and Lipson, D. (2017) Microbial community structure and soil pH correspond to methane production in Arctic Alaska soils. *Environ Microbiol* **19**: 3398–3410.

Walter, K. M., Chanton, J. P., Chapin, F. S., Schuur, E. A. G., and Zimov, S. A. (2008) Methane production and bubble emissions from arctic lakes: isotopic implications for source pathways and ages. *J Geophys Res* **113**: G00A08.

Walter, K. M., Zimov, S. A., Chanton, J. P., Verbyla, D., and Chapin, F. S. (2006) Methane bubbling from Siberian thaw lakes as a positive feedback to climate warming. *Nature* **443**: 71–75.

Wang, N. F., Zhang, T., Yang, X., Wang, S., Yu, Y., Dong, L. L., *et al*. (2016) Diversity and composition of bacterial community in soils and lake sediments from an Arctic lake area. *Front Microbiol* **7**: 1170.

Wendlandt, K.-D., Stottmeister, U., Helm, J., Soltmann, B., Jechorek, M., and Beck, M. (2010) The potential of methane-oxidizing bacteria for applications in environmental biotechnology. *Eng Life Sci* **10**: 87–102.

Wik, M., Varner, R. K., Anthony, K. W., MacIntyre, S., and Bastviken, D. (2016) Climate-sensitive northern lakes and ponds are critical components of methane release. *Nat Geosci* **9**: 99–105.

Winkel, M., Mitzscherling, J., Overduin, P. P., Horn, F., Winterfeld, M., Rijkers, R., *et al*. (2018) Anaerobic methanotrophic communities thrive in deep submarine permafrost. *Sci Rep* **8**: 1291.

Yang, S., Liebner, S., Winkel, M., Alawi, M., Horn, F., Dörfer, C., *et al*. (2017) In-depth analysis of core methanogenic communities from high elevation permafrost-affected wetlands. *Soil Biol Biochem* **111**: 66–77.

Yergeau, E., Hogues, H., Whyte, L. G., and Greer, C. W. (2010) The functional potential of high Arctic permafrost revealed by metagenomic sequencing, qPCR and microarray analyses. *ISME J* **4**: 1206–1214.

Yu, Z., and Chistoserdova, L. (2017) Communal metabolism of methane and the rare Earth element switch. *J Bacteriol* **199**: e00328-17.

in 't Zandt, M.H., Beckmann, S., Rijkers, R., Jetten, M.S. M., Manefield, M., and Welte, C.U. (2017) Nutrient and acetate amendment leads to acetoclastic methane production and microbial community change in a non-producing Australian coal well. *Microb Biotechnol* **11**: 626–638.

in 't Zandt, M.H., de Jong, A.E.E., Slomp, C.P., and Jetten, M. S.M. (2018) The hunt for the most-wanted chemolithoautotrophic spookmicrobes. *FEMS Microbiol Ecol* **94**: 1–17.

Supporting Information

Additional Supporting Information may be found in the online version of this article at the publisher's web-site:

Fig. S1. Map of the two sampled lakes in Utqiaġvik, Alaska, USA.

Fig. S2. Non-metric multidimensional scaling (NMDS) plot for archaeal community structure of reads from original cores 1–7 with a stress of 0.09.

Fig. S3. Non-metric multidimensional scaling (NMDS) plot for bacterial community structure of reads from original cores 1–7 with a stress of 0.02.

Fig. S4. Phylogenetic classification of amplified bacterial 16S rRNA genes in the methanogenic incubations. The maximum taxonomy depth is on family level. Taxonomic groups with < 2% abundance are grouped in 'Other'.

Fig. S5. Phylogenetic classification of amplified archaeal 16S rRNA genes in the methanotrophic incubations. The maximum taxonomy depth is on family level. Taxonomic groups with < 2% abundance are grouped in 'Other'.

Fig. S6. Rarefaction curves from bacterial reads in original core, singletons were removed.

Fig. S7. Rarefaction curves of archaeal reads in original cores, singletons were removed.

Fig. S8. Rarefaction curves of archaeal reads in methanogen enrichments, singletons were removed.

Fig. S9. Rarefaction curves of bacterial reads in methanotrophic enrichments, singletons were removed.

Table S1. GPS coordinates of the sediment core samples taken from Lake Emaiksoun and Unnamed Lake.

Table S2. Porewater data of 2 cores of Lake Emaiksoun (LE) and Unnamed Lake (UL) analyzed by inductive coupled plasma-optical emission spectrometry (ICP-OES) for aluminium (Al), calcium (Ca), iron (Fe), potassium (K), magnesium (Mg), manganese (Mn), sodium (Na), phosphorus (P), sulfur (S), silicon (Si), and zinc (Zn) in parts per million (ppm). Depth is shown in cm.

Table S3. Pore water data of 2 cores of Lake Emaiksoun (LE) and Unnamed Lake (UL) analyzed by continuous flow analysis (CFA) for nitrate (NO_3), ammonium (NH_4), phosphate (PO_4) and sodium (Na), potassium (K) and chloride (Cl) in $\mu mol\ L^{-1}$. Depth is shown in cm.

Table S4. Bacterial alpha diversity analyses. All data sets were rarefied for the smallest dataset = 35,769 sequences. Sample coverages were all above 80%, indicating that the communities were sampled deep enough.

Table S5. Archaeal alpha diversity analyses. All data sets were rarefied for the smallest dataset = 3,625 sequences. Sample coverages were all above 94%, indicating that the communities were sampled deep enough.

Table S6. Cell-specific rates for methane formation or oxidation calculated for the most active incubations.